Quenching Rate Constants of $NF(a^1\Delta)$ at Room Temperature

Kang Yan Du and D. W. Setser*

Department of Chemistry, Kansas State University, Manhattan, Kansas 66506 *(Received: June 22, 1989; In Final Form: October 16, 1989)*

The gas-phase quenching rate constants for $NF(a^1\Delta)$ have been measured at 300 K for 60 reagent molecules. The experiments were done in a Pyrex glass flow reactor coated with halocarbon wax using the 2F + HN_3 reaction as a source of $NF(a^1\Delta)$. The rate constants span a wide range of values; the rate constants for most diatomic molecules are less than 1×10^{-14} cm^3 molecule^{-1} s^{-1}, but more reactive molecules, such as C_2H_4, NH_3, or $P(CH_3)_3$, have rate constants near 10^{-11} cm^3 molecule^{-1} s^{-1}. For polyatomic reagents that can act as Lewis bases, a correlation was found between the magnitude of the quenching rate constant and the base strength (measured as the proton affinity) of the molecule, which is evidence that the closed-shell ($\pi_x^2-\pi_y^2$) component of the $NF(a^1\Delta)$ state is involved in the quenching. The rate constants for $NF(a^1\Delta)$ are larger than for the analogous $O_2(a^1\Delta)$ state because of the more attractive interaction potentials between NF(a) and stable reagent molecules. A few experiments were done at ~200 K to demonstrate that this NF(a) source is suitable for low-temperature studies; the rate constants for O_2, CO, and C_2H_4 decreased with reduction in temperature. The 300 K bimolecular self-removal rate constant for $NF(a^1\Delta)$ was assigned as $(5 \pm 2) \times 10^{-12}$ cm^3 molecule^{-1} s^{-1}; bimolecular energy pooling by NF(a) to give NF(b) is not an important quenching pathway. Quenching of NF(a) by F atoms has a small rate constant, $(4 \pm 2) \times 10^{-13}$ cm^3 s^{-1}.

Introduction

The first electronically excited state of NF (the $a^1\Delta$, 1.419 eV, state) is a potentially useful energy storage system because of its small radiative transition probability, 0.18 s^{-1}, and ease of chemical generation.[1-5] However, the NF(a → X) transition is sufficiently strong that the [NF(a)] can be conveniently monitored by observation of the 874-nm emission.[4-6] In the present work a comprehensive set of rate constants for the quenching of NF(a) at 300 K is presented. The method, which has been already described,[5,6] consists of generating NF(a) in the prereactor section of a flow reactor by the 2F + HN_3 reaction. The rate constant of the primary reaction[5]

$$HN_3 + F \rightarrow HF + N_3; \quad \Delta H° = -55 \text{ kcal mol}^{-1} \qquad (1)$$

is 1×10^{-10} cm^3 molecule^{-1} s^{-1}. On the basis of the nascent HF(v) vibrational distribution, the high yield of NF(a) from the secondary reaction,[5] and the observation of N_3 by LIF,[7] direct H abstraction giving N_3 has been assigned as the major channel. When $[F]_0$ is in 2-fold excess of $[HN_3]_0$, the secondary reaction gives NF(a) in nearly stoichiometric yield relative to $[HN_3]$.

$$N_3 + F \rightarrow NF(a) + N_2; \quad \Delta H° = -33 \text{ kcal mol}^{-1} \qquad (2)$$

The rate constant for (eq 2) was reported[5,6] by this laboratory as $(5 \pm 2) \times 10^{-11}$ cm^3 molecule^{-1} s^{-1} by measuring the variation of [NF(a)] along the flow reactor. This value is an order of magnitude greater than the one favored by Coombe et al.[8,9] In the present work a large value for k_2 was confirmed by observing the rise time of the NF(a) emission profile and the yield of NF(a) vs [F]; the preferred 300 K value seems to be $(4.0 \pm 1.5) \times 10^{-11}$ cm^3 molecule^{-1} s^{-1}. The NF(a) quenching studies described in this paper are an extension of our preliminary report.[6] The rate constants for NF(a) bimolecular self-destruction and quenching by HN_3, F atoms, N_2 and HF now have been determined, and the formation and decay kinetics of NF(a) in the 2F + HN_3 reaction system, both with and without added reagent, can be described with confidence at room temperature.

Our goal was to acquire a reliable set of NF(a) quenching rate constants at 300 K for stable molecules, and results for slightly more than 60 molecules are reported. The quenching rate constants of NF(a) are important for the development of energy storage systems and for comparison with similar species, such as $NH(a^1\Delta)$,[10] $CH_2(\tilde{a}^1A_1)$,[11] and $O_2(a^1\Delta)$.[12] The T_0 values for the NH, NF, O_2, and CH_2 states are 12 590, 11 442, 7880, and 2177 cm^{-1}, respectively. The NH(a) and $CH_2(\tilde{a})$ species react with saturated hydrocarbons by H abstraction and C–H insertion and by addition to unsaturated bonds,[10,11] whereas O_2(a) is quenched mainly by electronic-to-vibrational energy transfer (E–V) with very small rate constants.[12] We have used the magnitude of k_Q and the variation with deuterium substitution to discuss physical vs chemical quenching of NF(a). We will conclude that quenching occurs mainly by chemical reaction and that the potential arising from the $\pi_x^2-\pi_y^2$ electronic state component of the $NF(a^1\Delta)$ structure is more important than the potential from the $\pi_x\pi_y$ component. The quenching of NF(a) by Cl_2, Br_2, and I_2 also has been studied, but these large rate constants and associated results will be reported separately.[13]

Although not relevant to the present work, the uncertainty about k_2 has importance for the chemistry of N_3.[9,14,15] David and

(1) (a) Malins, R. J.; Setser, D. W. J. Phys. Chem. 1981, 85, 1342. (b) Bettendorff, M.; Klotz, R.; Peyerimhoff, S. D. Chem. Phys. 1986, 110, 315. (c) Yarkony, D. R. J. Chem. Phys. 1986, 85, 7261. (d) Becker, A. C.; Schurath, U. Chem. Phys. Lett. 1987, 142, 313.

(2) Clyne, M. A. A.; White, I. F. Chem. Phys. Lett. 1970, 61, 465.

(3) Pritt, A. T., Jr.; Patel, D.; Coombe, R. W. Int. J. Chem. Kinet. 1984, 16, 977.

(4) Cheah, C. T.; Clyne, M. A. A. J. Photochem. 1981, 95, 21.

(5) Habdas, J.; Wategaonkar, S.; Setser, D. W. J. Phys. Chem. 1987, 91, 451.

(6) Quinones, E.; Habdas, J.; Setser, D. W. J. Phys. Chem. 1987, 91, 5155. The quenching rate constant for F atoms was erroneously reported as 2×10^{-14} cm^3, s^{-1}, rather than 2×10^{-13} cm^3 s^{-1}.

(7) Beaman, R.; Nelson, T.; Richards, D. S.; Setser, D. W. J. Phys. Chem. 1987, 91, 6090.

(8) Coombe, R. D.; Pritt, A. T., Jr. Chem. Phys. Lett. 1978, 58, 606.

(9) (a) David, S. J.; Coombe, R. D. J. Phys. Chem. 1985, 89, 5206. (b) David, S. J.; Coombe, R. D. J. Phys. Chem. 1986, 90, 3260.

(10) (a) Cox, J. W.; Nelson, H. H.; McDonald, J. R. Chem. Phys. 1985, 96, 175. (b) Bower, R. D.; Jacoby, M. T.; Blauer, J. Chem. Phys. 1987, 86, 1955. (c) Drozdoski, W. S.; Baronarski, A. P.; McDonald, J. R. Chem. Phys. Lett. 1979, 64, 421. Chem. Phys. 1978, 30, 133. (d) Fueno, T.; Bonacic-Koutecky, V.; Koutecky, J. J. Am. Chem. Soc. 1983, 105, 5547. (e) Hack, W.; Wilms, A. J. Phys. Chem. 1989, 93, 3540. (f) Hack, W.; Wilms, A. Z. Phys. Chem. (Munich) 1989, 161, 107. (g) Freitag, F.; Rohrer, F.; Stuhl, F. J. Phys. Chem. 1989, 93, 3170. (h) Kajimoto, O.; Fueno, T. Chem. Phys. Lett. 1981, 80, 484. (i) Fueno, T.; Fukuda, M.; Yokoyama, K. Chem. Phys. 1988, 124, 265. (j) Kodama, S. J. Phys. Chem. 1988, 92, 5019.

(11) (a) Ashfold, M. N. R.; Fullstone, M. A.; Hancock, G.; Ketley, G. W. Chem. Phys. 1981, 55, 245. (b) Langford, A. O.; Petek, H.; Moore, C. B. J. Chem. Phys. 1983, 78, 6650. (c) Laufer, A. H. Rev. Chem. Intermed. 1981, 4, 225. (d) Hack, W.; Koch, M.; Wagener, R.; Wagern, H. Ber. Bungen-Ges. Phys. Chem. 1989, 93, 165.

(12) (a) Wayne, R. P. Singlet Oxygen; Frimes, A. A., Ed.; CRC Press: Cleveland, OH, 1984. (b) Singh, J. P.; Bacher, J.; Setser, D. W.; Rosenwaks, S. J. Phys. Chem. 1985, 89, 5347. (c) Wildt, J.; Bednarek, G.; Fink, E. H.; Wayne, R. P. Chem. Phys. 1988, 122, 463. (d) Huie, R. E.; Herron, J. T. Int. J. Chem. Kinet. 1972, 5, 197.

(13) Du, K. Y.; Setser, D. W., to be submitted for publication in J. Phys. Chem.

(14) Hershaw, T. L.; McDonald, M. A.; Stedman, D. H.; Coombe, R. D. J. Phys. Chem. 1987, 91, 2838.

(15) Hershaw, T. L.; McElwee, D.; Stedman, D. H.; Coombe, R. D. J. Phys. Chem. 1988, 92, 4606.

0022-3654/90/2094-2425$02.50/0

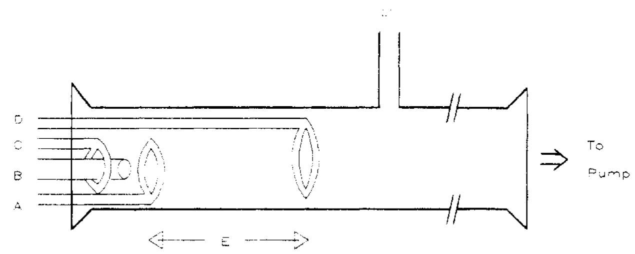

Figure 1. Schematic drawing of the 6.4 cm diameter flow reactor. A, B, C and D are the inlets for HN_3, F atoms, Ar buffer gas, and reagent, respectively; E denotes the prereactor section and F indicates pressure measurement. The distance between the HN_3 inlet and the reagent inlet was 20 cm. The entire reactor was coated with halocarbon wax.

Coombe[9] reported $k_2 = 1.8 \times 10^{-12}$ cm^3 s^{-1} by observing the $N_2(B \rightarrow A)$ emission along a flow reactor as a function of [F]. The $N_2(B)$ is produced from $N(^4S)$ reacting with N_3 and $N(^4S)$ is formed from interaction of N_3 with the reactor wall;[9] thus $[N_2(B)]$ should be proportional to $[N_3]$.[2] Coombe and co-workers also have reported emission from $PN(A^1\Pi \rightarrow X^1\Sigma^+)$[14] and $AsN(A^1\Pi \rightarrow X^1\Sigma^+)$[15] formed by the reaction of P or As atoms with N_3 that was generated by the reaction of F atoms with HN_3 in a flow reactor. According to our value of k_2, there is doubt about whether there would be enough N_3 radicals present to react with P and As, if $[F_0] > [HN_3]_0$. One explanation for the discrepancy may be the difficulty in reliably assigning high concentrations of F. Finding other mechanisms to explain the formation of $PN(A^1\Pi)$ and $AsN(A^1\Pi)$ seems unlikely.

Experimental Methods

A diagram of the flow reactor used to study the quenching of NF(a) is shown in Figure 1. The 150-cm-long, 6.4-cm-diameter reactor was coated with halocarbon wax (Halocarbon Products Corp.) to prevent the loss of the F, N_3, NF(a) and other radicals from interaction with the reactor wall. The flow rate of Ar carrier gas was typically 3 mmol s^{-1} at 2.4 Torr, corresponding to a linear flow velocity of 700 cm s^{-1} at 300 K. The flows of Ar buffer gas, HN_3, and F atoms were introduced at the entrance of the reactor. The reactor pressure was measured by a calibrated pressure transducer. A microwave discharge in a CF_4–Ar mixture ($\sim$10%) was used as the F atom source. The Ar flow, purified by passage through cooled (196 K) molecular sieve traps, was regulated by a needle valve and measured by a triflat flow meter that was calibrated with a wet test meter. The flow rates of CF_4 and HN_3 were obtained from the same pressure rise method as used for the reagents, vide infra. The reagent inlet ring was placed 20 cm downstream, giving a $\sim$30-ms period for reactions 1 and 2. Providing $[F]_0 = 2.3[HN_3]_0$ and $[HN_3]_0 \sim (0.5–1.5) \times 10^{12}$ molecule cm^{-3}, reactions 1 and 2 were complete at this point. For reagents with small quenching rate constants, thus requiring large flows, the reagent ring inlet was changed to an open-ended tube, 28 cm in length and 1.3 cm in diameter, to reduce the turbulence that was found when large flows of reagent gas were forced through the ring inlet.

The HN_3 was prepared by the reaction of 4:1 excess stearic acid with NaN_3 at 393 K under vacuum and stored as a 10% mixture in dry Ar in a Pyrex glass reservoir. Mass spectrometric analysis showed that the HN_3 was free of CO_2. Most reagents were taken from commercial sources and degassed and distilled with the middle fraction subsequently being stored in Pyrex reservoirs. The reagents having low vapor pressures or large quenching constants were prepared as dilute mixtures in Ar. Difficulties related to reagent purity are discussed when the data for a given reagent are presented. Reagent flow rates were monitored by means of pressure rise in a 5-L bulb with a 0–10 Torr MKS Baratron transducer.

The [F] was determined by either of two rapid titration reactions[16]

$$CF_3I + F \rightarrow CF_3 + IF; \quad k = 1.6 \times 10^{-10}\ \text{cm}^3\ \text{s}^{-1} \tag{3}$$

$$Cl_2 + F \rightarrow Cl + ClF; \quad k = 2.0 \times 10^{-10}\ \text{cm}^3\ \text{s}^{-1} \tag{4}$$

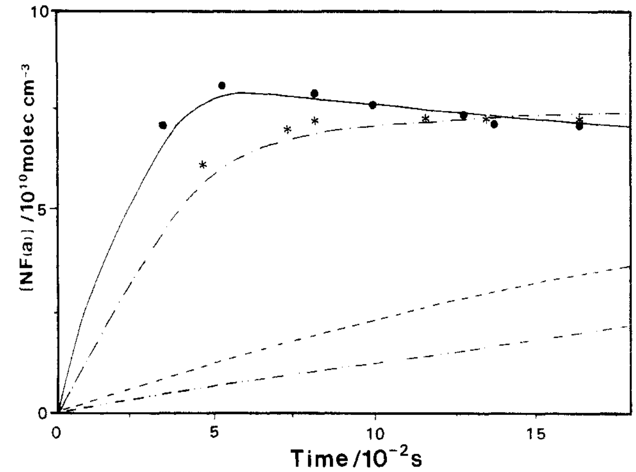

Figure 2. Concentration profiles for NF(a) along the flow reactor for $[HN_3]_0 = 8.2 \times 10^{10}$ molecules cm^{-3}: asterisk, $[F]_0 = 1.7 \times 10^{12}$; solid circle, $[F]_0 = 7.2 \times 10^{11}$ atoms cm^{-3}. The curves through these points are calculated results from numerical integration of the rate equations with rate constants given in the text, in particular, $k_2 = 4 \times 10^{-11}$ cm^3 molecule^{-1} s^{-1}. The [NF(a)] corresponding to the maximum NF(a–X) intensity was equated with $[HN_3]_0$. The curves at the bottom of the drawing are calculated results for the k_2 value of Coombe and co-workers[8,9] for the above concentrations.

The [F] was monitored by the HF($v = 3 \rightarrow 0$) emission intensity from the reaction of F atoms with C_2H_6.[5,17] The C_2H_6 was introduced into the flow reactor 15-cm downstream from the inlet used for CF_3I or Cl_2, corresponding to a reaction time of 22 ms for the titration reactions. The HF($v = 3 \rightarrow 0$) emission was observed immediately after the position for addition of C_2H_6. Since the reaction of CF_3 or Cl with F in the system is negligible, the reduction of HF($3 \rightarrow 0$) emission intensity caused by addition of CF_3I or Cl_2 can be associated with the removal of [F]. The plots of the HF($3 \rightarrow 0$) intensity versus the added $[CF_3I]$ or $[Cl_2]$ were linear when [F] was in excess. However, the plots gradually became flat when the $[Cl_2]$ or $[CF_3I]$ approached $[F]_0$, which made assigning the absolute [F] concentration from the $[CF_3I]$ or $[Cl_2]$ difficult. This problem was overcome by simulating the [F] curves by numerical integration of the rate equations with the given experimental conditions and known rate constants. The computer fits to the experimental results allowed $[F]_0$ to be obtained. As in previous work,[4] the $[F]_0$ was 2-fold larger than the $[CF_4]$ if $[CF_4]$ was $\leq 1 \times 10^{12}$ molecule cm^{-3}; however, the dissociation efficiency was reduced for higher CF_4, and $[F]_0$ was approximately equal to the $[CF_4]$ for concentrations $\geq 3 \times 10^{12}$ molecules cm^{-3}.

The detection system was a 0.5-m monochromator (Minuteman) with a 500-nm blazed grating and a cooled RCA-C31034 photomultiplier tube (PMT). The signals were recorded with a photon counter and displayed on a strip chart recorder. The wavelength response of the monochromator and the PMT was calibrated with a standard quartz-I_2 lamp and confirmed by measuring the rotational transitions of the HF($v = 3 \rightarrow v = 0$) band in the 840–890 nm range. The NF(a–X) spectrum consists of a main peak with red- and blue-shifted wings; the relative [NF(a)] was monitored at 874 nm, using a slit width of 1 mm. The monochromator was mounted on a table with wheels so that observations could be made along the flow reactor.

Experimental Results

(*1*) *Formation and Decay of NF(a) in Absence of Q.* Figure 2 shows some typical NF($a \rightarrow X$) emission intensity profiles vs the reaction time for excess $[F]_0$ with $[HN_3]_0 = 8.2 \times 10^{10}$ molecule cm^{-3}. Emission profiles for higher $[HN_3]_0$ concentrations

(16) (a) Clyne, M. A. A.; McKenney, D. J.; Walker, K. F. *J. Chem. Soc., Faraday Trans. 2* **1973**, *69*, 3596. (b) Bozelli, J. W.; Kaufman, M. *J. Phys. Chem.* **1973**, *72*, 1748.

(17) Agrawalla, B. S.; Setser, D. W. In *Gas Phase Chemiluminescence and Chemi-ionization*; Fontijn, A., Ed.; Elsevier: New York, 1985.

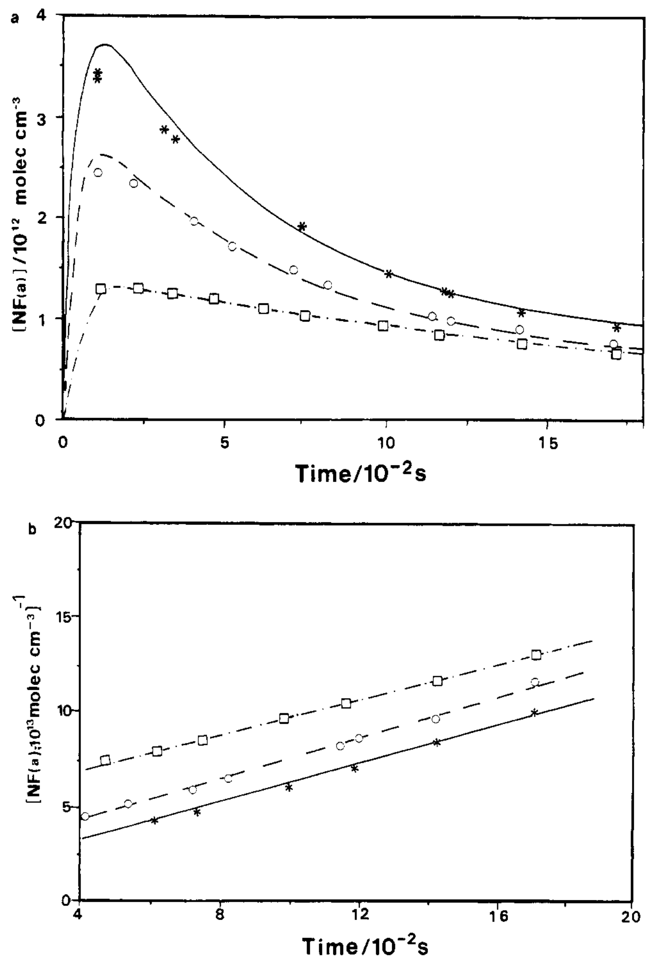

Figure 3. (a) Plot of [NF(a)] vs time for large [NF(a)]: □, $[HN_3]_0 = 1.5 \times 10^{12}$ and $[F]_0 = 7.5 \times 10^{12}$; O, $[HN_3]_0 = 3.2 \times 10^{12}$ and $[F]_0 = 1.3 \times 10^{13}$; *, $[HN_3]_0 = 4.9 \times 10^{12}$ and $[F]_0 = 1.3 \times 10^{13}$ molecules cm^{-3}. The smooth curves are the calculated results from numerical integration of the rate equations with rate constants given in the text, the critical value is $k_6 = 5.0 \times 10^{-12}$ cm^3 molecule^{-1} s^{-1}. (b) Plot of $[NF(a)]^{-1}$ vs time from the experiments in part a. The absolute NF(a) concentrations were assigned as described in Figure 3a. The second-order plots were made only for times after the maximum NF(a) concentration was reached.

are shown in Figure 3. In order to measure quenching rate constants, [NF(a)] should be approximately constant along the length of the reactor in the absence of reagent, and these conditions are discussed first. The HN_3 is converted to N_3 in less than 10 ms for conditions of excess $[F]_0$, since k_1 is 1×10^{-10} cm^3 s^{-1}. The rise time of the NF(a) emission profile is mainly associated with the rate of the reaction between F atoms and N_3 and increasing $[F]_0$ moves the maximum to shorter times for fixed $[HN_3]_0$. Simulating the characteristic [NF(a)] profiles versus time shown in Figure 2 suggests $k_2 \approx (4.0 \pm 1.5) \times 10^{-11}$ cm^3 s^{-1}. Furthermore, the [NF(a)] obtained for conditions such that $[F]_0 \leq [HN_3]_0$ also requires a rate constant of this magnitude; the NF(a) yield for such conditions depends on the competition between N_3 and HN_3 for F atoms. If Coombe et al.'s value of 1.8×10^{-12} cm^3 s^{-1} is used for $[F]_0 = 1.7 \times 10^{12}$ and $[HN_3]_0 = 8.2 \times 10^{10}$ molecules cm^{-3}, the maximum for [NF(a)] would appear much later; see Figure 2. Our NF(a) profiles are incompatible with such a small value for k_2.

The [NF(a)] decays along the reactor for large excesses of either [F] or $[HN_3]$ or high [NF(a)]. The rate constant for quenching NF(a) by F atoms was reported previously[6] as $\sim 2 \times 10^{-13}$ cm^3 s^{-1}; a variety of new experiments, like those shown in Figure 2 for a range of $[F]_0$, favor $(4 \pm 2) \times 10^{-13}$ cm^3 s^{-1}, and the higher value is preferred. The rate constant for quenching of NF(a) by HN_3 is $(2.1 \pm 1.0) \times 10^{-13}$ cm^3 s^{-1}, as measurements to be presented in a later section using HN_3 as a reagent will show. The similar NF(a) decay profiles for comparable excesses of [F] and $[HN_3]$ also demonstrated that the quenching rate by HN_3 is similar to that for F atoms.

With $[F]_0 \geq 2.3[HN_3]_0$ and $[HN_3]_0 < 5 \times 10^{11}$ molecules cm^{-3}, the NF(a) intensity declined to only 90–95% of the maximum intensity after a flow time of 0.18 s. For this concentration range the CF_2, N_2, HF, CF_4, and impurities in Ar do not cause significant quenching. Since the radiative decay rate[1] ($\tau^{-1} = 0.18$ s^{-1}) is negligible and self-quenching can be neglected at $[NF(a)] \leq 5 \times 10^{11}$ molecules cm^{-3}, the wall deactivation of NF(a) on the halocarbon-wax-coated vessel is the dominant loss process. The data in Figure 2 correspond to $k_W < 0.15$ s^{-1}, which is in agreement with the earlier report.[6] These conditions thus define the $[F]_0$ and $[HN_3]_0$ concentration range for which our apparatus can be used to study quenching by adding reagent to the flow reactor.

For low [F] the N_3 self-destruction reaction

$$N_3 + N_3 \rightarrow 3\,N_2 \tag{5}$$

is in competition with reaction 2 in the prereactor. For the $[HN_3]_0$ employed in this work, $(0.5–2.0) \times 10^{-12}$ molecules cm^{-3}, the NF(a $\rightarrow$ X) emission profile was insensitive to the rate constant for reaction 5. More direct measurements by Marinelli[18] suggest a rate constant of 2.4×10^{-12} cm^{-3} s^{-1} and eq 5 becomes important for $[N_3] \geq 10^{13}$ molecules cm^{-3}.

(*2*) *Bimolecular Self-Destruction and the Energy Pooling Reactions of NF(a)*. A self-destruction rate constant of $(2.2 \pm 1.2) \times 10^{-12}$ cm^3 s^{-1}, defined as $-d[NF(a)]/dt = k[NF(a)]^2$, was previously reported from a limited data set[6]

$$NF(a) + NF(a) \rightarrow N_2 + 2F \text{ (or } F_2) \tag{6a}$$

$$\rightarrow 2NF(X) \text{ (or } NF(X) + NF(a)) \tag{6b}$$

$$\rightarrow NF(X) + NF(b) \tag{6c}$$

Since this rate constant is crucial for energy storage systems involving NF(a), new data were acquired for $[HN_3] = (0.6–2.0) \times 10^{12}$ molecules cm^{-3} for conditions of excess [F]. Freshly prepared HN_3 was used and the absence of CO_2 or other impurities was confirmed by mass spectrometry. To obtain the rate constant for reaction 6, the absolute [NF(a)] is needed. It has been shown[5] that the [NF(a)] is $\geq 0.85[HN_3]_0$ in the $2F + HN_3$ system for excess $[F]_0$ and low $[HN_3]_0$. Since no special precautions were taken regarding HN_3 purity in that work and no adjustments were made for quenching, we believe that the efficiency is higher than 0.85. The data of Figure 3 are self-consistent in the sense that the maximum NF(a $\rightarrow$ X) intensity values scale in proportion to the $[HN_3]_0$. However, with increase of $[HN_3]_0$ reaction 6 becomes important and the NF(a) formation and removal steps are not completely separated in time. Therefore, the [NF(a)] never reaches the equivalent of $[HN_3]_0$. In order to make the second-order plot in Figure 3b, the [NF(a)] was assigned from the observed maximum NF(a–X) intensity and scaled according to the relative emission intensity from the low $[HN_3]_0$ data of Figure 2 for which the maximum [NF(a)] was taken as $[HN_3]_0$. The plot of $[NF(a)]^{-1}$ versus the reaction time, Figure 3b, supports second-order kinetics and gives a rate constant of $(5.0 \pm 2.0) \times 10^{-12}$ cm^3 s^{-1}, which is about 2 times larger than that reported previously.[6] This rate constant is difficult to assign because of the uncertainty in the absolute NF(a) concentration. We prefer the larger rate constant because the more extensive data follow second-order kinetics for a larger [NF(a)] range. In order to investigate the possible pressure dependence of k_6, the results for 2 Torr were compared to experiments at 7 Torr, but no change in k_6 was found.

The $O_2(^1\Delta_g)$ energy pooling reaction has been a subject of intense interest, and the component giving $O_2(X) + O_2(b)$ has a rate constant of 2×10^{-17} cm^3 s^{-1}.[12a] The analogous process for NF(a) is represented by eq 6c with a rate constant k_{EP}. A characteristic greenish "afterglow" from the NF(b $\rightarrow$ X) transition was observed downstream from the HN_3 inlet. This emission, which is fairly strong in the mixing zone of the prereactor, gradually decreased and reached a constant low level in the reactor.

(18) Marinelli, W. J., private communication, 1988.

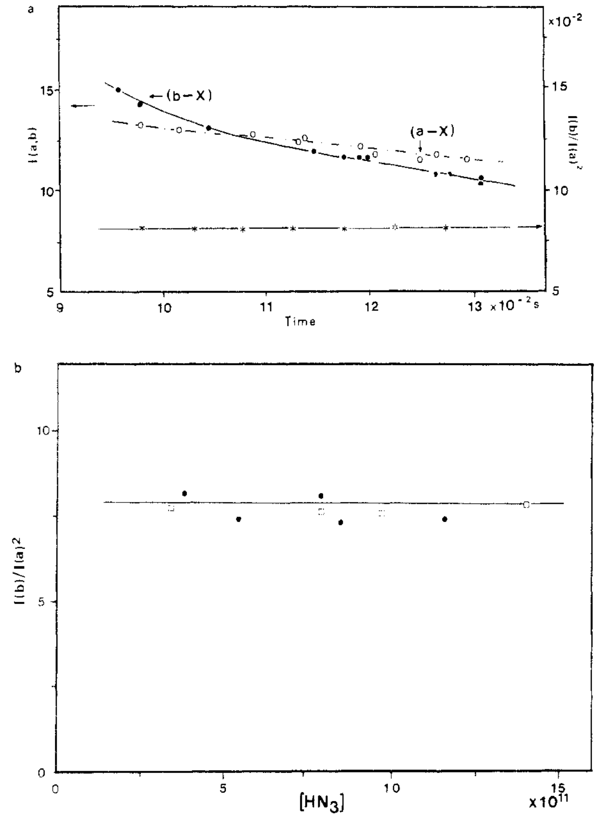

Figure 4. (a) Plot of the steady-state NF(b–X) intensity along the flow reactor for [NF(a)] = 8 × 10^{11} molecules cm^{-3}: ○, NF(a–X) intensity; ●, NF(b–X) intensity; *, $I(b)/I(a)^2$. The intensity scales are arbitrary. (b) Comparison of the intensity ratio $I(NF(b))/I(NF(a))^2$ vs $[HN_3]_0$ after 150-ms reaction time. The [NF(a)] is proportional to $[HN_3]_0$; ●, $[CF_4]$ = 2.4 × 10^{12} molecules cm^{-3}; □, $[CF_4]$ = 1.1 × 10^{12} molecules cm^{-3}.

The early afterglow arises from energy transfer between HF(v ≥ 2) and NF(a);[19] the downstream afterglow was attributed to reaction 6c, because the [HF(v = 2–3)] is negligible downstream of the F + HN_3 reaction zone. Since the radiative decay rate (τ_b = 19 ms)[19,20] of NF(b) is faster than the rate of formation, [NF(b)] acquires the steady-state concentration described by eq 7, providing that wall quenching of NF(b) can be ignored. The

$$[NF(b)] = k_{EP}[NF(a)]^2/\tau^{-1} \quad (7)$$

proportionality of [NF(b)] to $[NF(a)]^2$ demonstrated in Figure 4 for time and [NF(a)] as variables, confirms that NF(b) is formed by energy pooling. In order to obtain k_{EP}, we compared the ratio (R_{ab}) of the integrated emission intensities for NF(a) and NF(b); $R_{ab} = \tau_a^{-1}[NF(a)]\beta_a/\tau_b^{-1}[NF(b)]\beta_b$, β_a and β_b are the monochromator responses at 526 and 874 nm and τ_a and τ_b are the lifetimes of the a and b states, 5.6 s and 19 ms, respectively. The rate constant, k_{EP}, is given by eq 8. The absolute [NF(a)] at

$$k_{EP} = \frac{\tau_a^{-1}\beta_a}{R_{ab}[NF(a)]\beta_b} \quad (8)$$

the observation point was assigned from the ratio of the intensities at the maximum of the [NF(a)] profile and at the observation point. Results from several experiments are listed in Table I for different $[F]_0/[HN_3]_0$. The mean value is k_{EP} = (5.7 ± 1.0) × 10^{-15} cm^3 s^{-1}, and eq 6c is a minor part of the total self-destruction of NF(a). Reaction 6c is exothermic by about 3894 cm^{-1} and excitation to NF(b, v' = 5) is possible; however, only NF(b, v' = 0) was observed. In contrast with NF(a), ≈50% of the second-order decay of O_2(a) gives O_2(b) with an unusual vibrational distribution v_0,v_1,v_2 = 0.5:0.06:1.[21,22]

TABLE I: Rate Constant for Energy Pooling by NF(a)

expt	R_{ab}	[NF(a)], molecules cm^{-3}	k_6(obsd), 10^{-15} cm^3 s^{-1}
1	7.3	3.7 × 10^{11}	5.6
2	7.7	4.1 × 10^{11}	4.9
3	9.1	3.4 × 10^{11}	5.0
4	4.4	5.6 × 10^{11}	6.3
5	5.3	6.0 × 10^{11}	4.9
6	4.6	5.6 × 10^{11}	6.1
7	7.0	3.0 × 10^{11}	7.4
			mean 5.7 (±1.0)

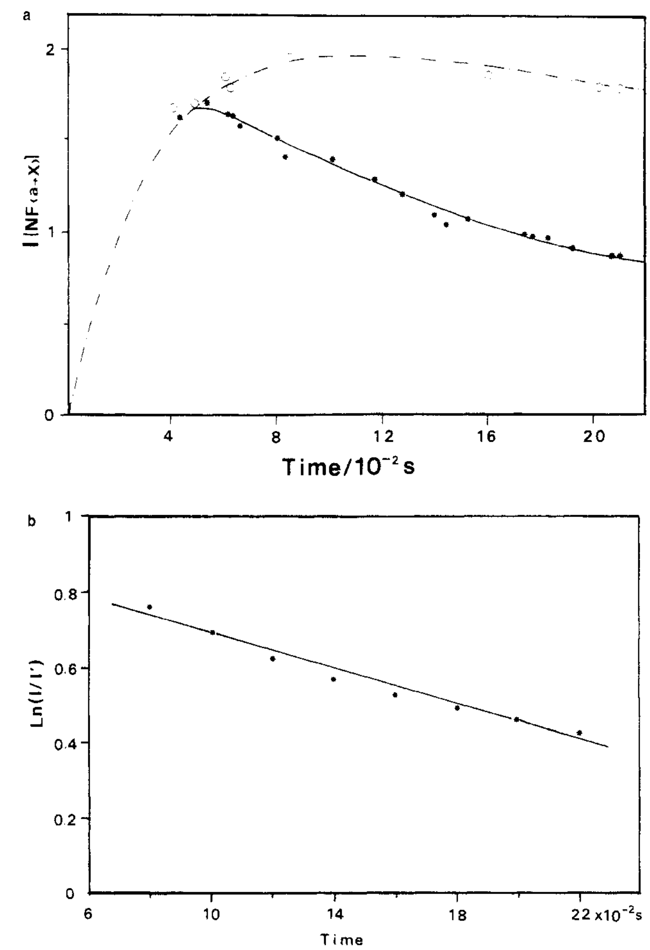

Figure 5. (a) Comparison of the decay of NF(a) in a coated (○) and uncoated (●) reactor for [NF(a)] = ~5 × 10^{11} molecules cm^{-3} and 3 Torr pressure. (b) A logarithmic comparison of the [NF(a)] in the coated and uncoated flow reactor versus reaction time. See text for details.

A search was made for the equivalent of the O_2(a) "dimols" emission,[23-25] reaction 9, which should be at ~437 nm.

$$NF(^1\Delta) + NF(^1\Delta) \rightarrow 2NF(^3\Sigma^-) + h\nu(437\ nm) \quad (9)$$

No emission could be observed for [NF(a)] ≤ 2 × 10^{12} molecules cm^{-3}.

(3) *Deactivation of NF(a) by Pyrex*. All previous experiments in our laboratory with the F/HN_3 system have utilized halocarbon wax coated reactors[4,6] to inhibit the loss of F, N_3, and NF(a) by interaction with the walls. In order to ascertain the loss of NF(a)

(19) Habdas, J.; Setser, D. W. J. Phys. Chem. 1988, 93, 229.
(20) (a) Cha, H.; Setser, D. W. J. Phys. Chem. 1987, 91, 3758; 1989, 93, 235. (b) Bao, X.; Setser, D. W. J. Phys. Chem. 1989, 93, 8162.
(21) Schurath, U. J. Photochem. 1975, 4, 215.
(22) Fisk, G. A.; Hays, G. N. J. Chem. Phys. 1982, 77, 4965.
(23) (a) Benard, D. J.; McDermott, W. E.; Pchelkin, N. R.; Bousek, R. R. Appl. Phys. Lett. 1979, 34, 40. (b) Bader, L. W.; Ogryzlo, E. A. Discuss. Faraday Soc. 1964, 37, 46.
(24) Khan, A. U. In Singlet Oxygen; Frimes, A. A., Ed.; CRC Press: Cleveland, OH, 1984.
(25) Billington, A. P.; Borrell, P.; Rich, N. H. J. Chem. Soc., Faraday Trans. 2 1988, 84, 727.

on bare Pyrex walls, an uncoated glass reactor of similar size to the one shown in Figure 1 was installed. However, the 24-cm-long prereactor section was coated with the halocarbon wax so that the $2F + HN_3$ reaction could be completed. The decay of the NF(a) emission along the uncoated reactor for $[HN_3]_0 = 6.4 \times 10^{11}$ and $[F]_0 = 1.3 \times 10^{12}$ molecules cm^{-3} at 3 Torr is shown in Figure 5; the bimolecular self-destruction rate is negligible for this [NF(a)]. In order to find the deactivation constant, k_W, we compared the decay rates for the coated (eq 10a) and uncoated (eq 10b) reactors at each reaction time; the cumulative gas-phase quenching is denoted by $k_C[C]$. The slope of the intensity ratios

$$\ln [NF(a)]_{t_2}' - \ln [NF(a)]_{t_1}' = -k_C[C]\,\Delta t \qquad (10a)$$

$$\ln [NF(a)]_{t_2} - \ln [NF(a)]_{t_1} = -(k_C[C] + k_W)\Delta t \qquad (10b)$$

$$\ln\left(\frac{[NF(a)]}{[NF(a)]'}\right)_{t_2} - \ln\left(\frac{[NF(a)]}{[NF(a)]'}\right)_{t_1} = -k_W\,\Delta t \qquad (10c)$$

vs reaction time in Figure 5b gives $k_W = 2.8 \pm 0.5$ s^{-1}. These experiments showed that a coated Pyrex reaction vessel is essential for studying the homogeneous decay kinetics of NF(a).

The rate constant, k_w, can be related to the deactivation efficiency at the wall by using the equation given by Wayne[12a] for $O_2(a)$.

$$k_w = \left(\frac{r^2P}{8D_0} + \frac{2r}{\gamma\bar{u}}\right)^{-1} \qquad (10d)$$

In this equation $\bar{u}$ is the mean molecular velocity, r is the radius of the flow reactor, γ is the deactivation probability at the Pyrex wall, P is pressure, and D_0 is the diffusion constant. We used 150 Torr cm^2 s^{-1} as D_0, which was taken as the diffusion constant for O_2 in Ar. For 3 Torr pressure the first term contributes less than 10% and the deactivation efficiency can be evaluated by using only the last term. Since $\bar{u} = 5.9 \times 10^4$ s^{-1} and $r = 3.2$ cm, $\gamma = 3 \times 10^{-4}$. This value, which probably will depend to some extent upon the history of the Pyrex surface, is approximately 30 times greater than for $O_2(a)$ on Pyrex surfaces.[12a]

(4) Quenching Rate Constants of NF(a) at Room Temperature. The quenching of NF(a) with added reagent can be described by the following reactions and equations; the total rate constant is $k_Q = k_{Qa} + k_{Qb}$:

$$NF(a) + Q \xrightarrow{k_{Qa}} NF(X) + Q^*$$
$$\xrightarrow{k_{Qb}} \text{reactive channels} \qquad (11)$$

For low NF(a) concentration the differential rate law is given by eq 12 with k' representing the total first-order deactivation in the

$$d[NF(a)]/dt = (k_Q[Q] + k')[NF(a)] \qquad (12)$$

absence of Q. For high [NF(a)], the bimolecular self-destruction reaction would add a second-order term to eq 12 and seriously complicate the rate equation. Therefore, rate constants were measured with $[NF(a)] \leq 0.6 \times 10^{12}$ molecules cm^{-3} by monitoring the loss of NF(a) under the conditions such that [Q] was in excess over [NF(a)]. The integrated pseudo-first-order rate law can be written as eq 13; t is the reaction time corresponding

$$\ln [NF(a)] = -(k_Q[Q] + k')t + \text{const} \qquad (13)$$

to the distance between the reagent inlet and observation point. The relative [NF(a)] was monitored by the NF(a–X) emission intensity at 874.0 nm, for conditions such that k' was negligible. The rate constants were measured by changing [Q] with observation of NF(a) at a fixed point for 2–3 Torr of Ar. Two or three fixed reaction times were used for most reagents. In order to reduce systematic error, the relative [NF(a)] was measured with random ordering of [Q], and the slopes were analyzed by using a least-squares fit. For some reagents the possibility of monomer $\Leftrightarrow$ dimer equilibrium must be considered in calculating the flow rates. One case was CF_3COOH vs $(CF_3COOH)_2$,[26] since the

(26) Taylor, M. D.; Templeman, M. B. *J. Am. Chem. Soc.* **1956**, *78*, 2950.

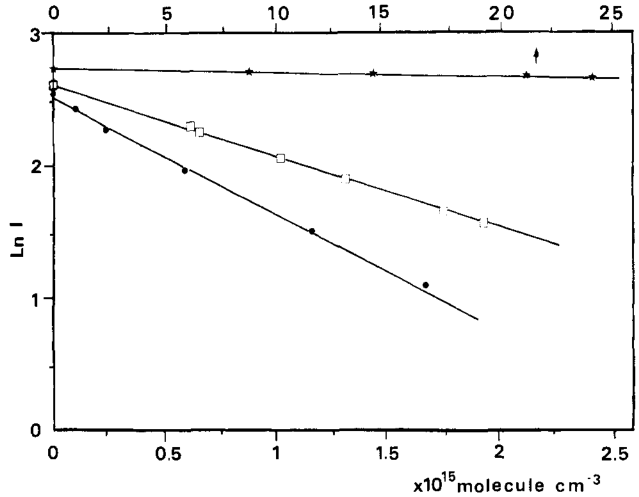

Figure 6. Representative pseudo-first-order NF(a) quenching plots for some diatomic reagents. The reaction times were 0.253, 0.175, and 0.153 s for N_2 (*), CO (□), and O_2 (●), respectively. The $[F]_0$ and $[HN_3]_0$ were (26 and 3.8, 17 and 2.6, 20 and 7) $\times 10^{11}$ molecules cm^{-3} for the N_2, CO, and O_2 experiments, respectively.

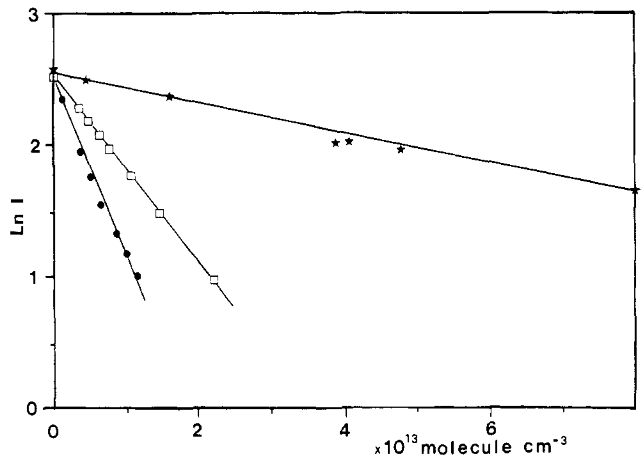

Figure 7. Representative pseudo-first-order NF(a) quenching plots for some organic reagents: (*, CH_3Br) Δt = 47 ms with $[HN_3]_0$ and $[F]_0$ = (6 and 14) $\times 10^{11}$ molecules cm^{-3}; (□, CH_3CHCH_2) Δt = 60.3 ms with $[HN_3]_0$ and $[F]_0$ (2.3 and 30) $\times 10^{11}$ molecules cm^{-3}; (●, CH_3I) Δt = 47 ms with $[HN_3]_0$ anmd $[F]_0$ = (5 and 17) $\times 10^{11}$ molecules cm^{-3}.

equilibrium constant is 4.3 at 300 K. At 200 Torr, the pressure in the storage reservoir, the monomer to dimer ratio is 0.03. But, in the reactor and the vessel used to measure the pressure rise, the partial pressure was less than 0.05 Torr, and the dimer was completely dissociated. Typical quenching plots are shown in Figures 6 and 7; the linearity confirms pseudo-first-order kinetics. The slopes of these plots give $k_Q\Delta t$; the reaction time was obtained from $x/\langle v\rangle$. The CH_3COCH_3, CH_3OH and NH_3 reactions were chosen as reference, and these rate constants were measured several times during the 14-month period of data collection; the deviation from the average was less than ±10%. The room temperature rate constants are summarized in Tables II–IV; the previously reported results for NF(a),[6] as well as the constants for NF(b),[20] $O_2(a)$,[12] and NH(a)[10] are listed for comparison. The rate constants are grouped according to diatomic and triatomic molecules, simple organic molecules, and molecules containing group V elements for ease of discussion.

The quenching rate constants for diatomic and triatomic molecules, which are listed in Table II, are in the range of 10^{-16}–10^{-14} cm^3 s^{-1}, with the exception of H_2S and ClF. In order to determine the rate constant for such slow rates, high reagent concentrations were required and some experiments were done with the valve to the pump partially closed so that the reaction time was doubled. For reagents with small rate constants, impurities and/or improper operating conditions can introduce error, and for several reagents the new rate constants are smaller than

TABLE II: Quenching Rate Constants by Diatomic and Triatomic Molecules

reagent	NF(a),[a,b] 10^{-14} cm^3 s^{-1}	NF(b),[c] 10^{-14} cm^3 s^{-1}	O_2(a),[e] 10^{-18} cm^3 s^{-1}	NH(a),[f] 10^{-11} cm^3 s^{-1}
N_2	<0.0012 (<0.013)	0.09 ± 0.03	0.1	0.0075 ± 0.006
CO	0.36 ± 0.04 (0.63)	0.21 ± 0.05	9.0 ± 3.0	1.35 ± 0.07
O_2	0.70 ± 0.07 (0.66)	2.4 ± 0.3	1.9 ± 0.5	0.0045 ± 0.0005
NO	<0.15 (0.05)	1.3 ± 0.4	50 ± 10	3.0 ± 0.5
H_2	0.007 ± 0.002	2.5 ± 0.3	4.5 ± 0.5	0.29 ± 0.04
HF	(0.3)	80 ± 15	140 ± 50	0.073 ± 0.026
HCl	0.16 ± 0.03	1.8 ± 0.7	4 ± 3	7.9 ± 0.8
F_2	(3.2)	380 ± 50		0.063 ± 0.016
ClF	770 ± 70	480 ± 100		
CO_2	0.006 ± 0.002	0.14 ± 0.02	0.5	0.025 ± 0.002
N_2O	0.010 ± 0.003	0.1 ± 0.052	0.075	0.16 ± 0.01
H_2O	4 ± 1	86 ± 8	5.6 ± 0.4	
D_2O	4 ± 1	2.2 ± 0.3		
SO_2	4.3 ± 0.5	0.09 ± 0.04	~5	
COS[d]	6 ± 2	1.1 ± 0.3	2 ± 1	
H_2S	61 ± 6	2.9 ± 0.3	2 ± 1.5	
NO_2	0.65 ± 0.10			

[a] The rate constants in parentheses were taken from ref 6; the rate constants previously reported for H_2 and D_2 are in error, see text. [b] The error limits are the standard deviation from multiple experiments; but if systematic error was suspected, the error limits were increased. The error generally is larger for the smaller rate constants. [c] Taken from ref 20. [d] Good first-order quenching plots were not obtained. The listed rate constants are from the second part of the decay plots. [e] See ref 12a and b. [f] See ref 10b–f; the recent study by Hack and Wilms has resulted in a 100-fold reduction for k_{O_2}, but confirmation for k_{NO} and k_{N_2}.

TABLE III: Quenching Rate Constants for Organic Molecules

reagent	NF(a),[a,b] 10^{-14} cm^3 s^{-1}	NF(b),[c] 10^{-14} cm^3 s^{-1}	O_2(a),[e] 10^{-18} cm^3 s^{-1}	NH(a),[f] 10^{-11} cm^3 s^{-1}
SF_6	<0.01	1.1 ± 0.2	<0.01	
CF_4	(≤0.005)	0.6 ± 0.3	0.38 ± 0.04	
CH_4	<0.01	16 ± 3	1.4 ± 0.3	0.38 ± 0.1
C_2H_6	0.07 ± 0.02	14 ± 2		1.2 ± 0.5
C_3H_8	0.10 ± 0.02 (0.59)	26[d]	2.4 ± 0.2	4.2 ± 0.5
CH_3CN	0.55 ± 0.05	22 ± 3		
CD_3CN	0.49 ± 0.05	0.35 ± 0.10		
CH_3Cl	1.1 ± 0.2 (2.5)	20 ± 2	5 ± 2	
CH_3Br	26 ± 4	20.3 ± 0.5	30 ± 15	
CH_3I	230 ± 20	36 ± 5	40 ± 20	
CH_3OH	11 ± 1	67 ± 7		
CH_3OD	10 ± 1	20 ± 2		
CH_2Cl_2	0.71 ± 0.08	16 ± 2		
CD_2Cl_2	0.61 ± 0.07	0.47 ± 0.05		
CH_2Br_2	17 ± 2	21 ± 3		
CHF_3	0.027 ± 0.003	11 ± 1		
$CHCl_3$	0.51 ± 0.03	6.4 ± 1.7		
$CDCl_3$	0.30 ± 0.03	0.3 ± 0.1		
CF_2ClBr	0.59 ± 0.06			
CF_2Br_2	0.94 ± 0.08			
CF_3I	24 ± 3	0.5 ± 0.1	<0.5	
CCl_4	0.39 ± 0.02	1.2 ± 0.2		
C_2H_2	23 ± 2	4.2 ± 0.2	6 ± 0.6	
C_2H_4.	32 ± 3 (30)	11 ± 1	2.0 ± 0.2	8.8 ± 0.8
C_2H_3Cl	16 ± 2			
CH_2CF_2	12 ± 2			
CH_3CHCH_2	150 ± 20	16 ± 6	2.2 ± 0.2	3.6 ± 0.4[f]
C_4H_6	270 ± 30		10 ± 5	(f)
$(CH_3)_2CO$	37 ± 2	26 ± 4	1.6 ± 0.4	
$(CD_3)_2CO$	33 ± 4	0.55 ± 0.06		
CF_3COOH	57 ± 6	31 ± 5	<5	
$(CF_3)_2CO$	0.028 ± 0.002			
CH_3OCH_3	130 ± 15			
$C_2H_5OC_2H_5$	140 ± 15			

[a] The rate constants in parentheses were taken from ref 6. [b] The error limits are the standard deviation from multiple experiments, but if systematic error was suspected, the error limits were increased. [c] Taken from ref 20. [d] This rate constant actually is for cyclopropane rather than propane. [e] See ref 12 parts a, b, and d. [f] See ref 10a–f; the rate constant for *cis*-butene is 25 × 10^{-11} cm^3 s^{-1}, ref 10b. On the basis of the newer work, the rate constant for propene probably should be increased.

those from the early work. One reason is that the reagent inlet design used previously was a poor choice for large reagent flows (reagents with small k_Q). High flows through the small holes of the ring forced the reagent gas *upstream*. This was especially serious for reagents which react with F atoms, because the loss of F atoms from the prereactor prevented NF(a) formation, as well as generated radicals that could quench NF(a). For reagents with $k_Q > 0.5 \times 10^{-14}$ cm^3 s^{-1}, the earlier results should be reliable. In this context the rate constants for O_2 and C_2H_4 were confirmed and the new result for CO is, within the combined uncertainty of the two measurements, equal to the prior value. Nevertheless, the chemical environment in the flow reactor is complex and the data must be regarded with care for each reagent.

New measurements were made with higher purity CO and N_2. Although the rate constants for CO and N_2 obtained in this work are smaller than those given in the previous report,[6] especially

TABLE IV: Quenching Rate Constants by Molecules of Group V Atoms

reagent	NF(a),[a,b] 10^{-14} cm^3 s^{-1}	NF(b), 10^{-14} cm^3 s^{-1}	O_2(a),[d] 10^{-18} cm^3 s^{-1}	NH(a),[e] 10^{-11} cm^3 s^{-1}
NF_3	0.025 ± 0.005	0.34 ± 0.15		
HN_3	21 ± 2			12.0 ± 0.6
NH_3	360 ± 20 (190)	8.8 ± 0.9	10 ± 2	11.0 ± 0.8
ND_3	360 ± 19	2.5 ± 0.5		
NH_2CH_3	1250 ± 200	37 ± 4	13 ± 2	
$NH(CH_3)_2$	1750 ± 100		93 ± 6	
$N(CH_3)_3$	2600 ± 200 (1300)		3000 ± 500	
PCl_3	210 ± 20	0.2		
PH_3	560 ± 60			
$P(CH_3)_3$	2300 ± 200			
$Bi(CH_3)_3$	2700 ± 200	48 ± 5		
CF_3NO	(800)	55 ± 5	$(3 \pm 1) \times 10^6$	

[a] The rate constants in parentheses were taken from ref 6. [b] The error limits are the standard deviation from multiple experiments or ±10%, whichever is the larger. [c] Taken from ref 20. [d] See ref 12a,b. [e] See ref 10b,c.

for the N_2, the 2 orders of magnitude difference between k_{CO} and k_{N_2} is confirmed. In fact, even the present measurements probably give only an upper limit value to k_{N_2}. We remeasured k_{NO} with the open inlet tube design and observed a dependence on the purity of NO. After repeated distillation a value of 0.15×10^{-14} cm^3 s^{-1} was obtained and this is quoted as an upper limit, since the earlier study obtained even a smaller value. Nitrogen dioxide also was studied because it is a free radical and is the common impurity in NO. The rate constant for NO_2 is 0.65×10^{-14} cm^3 s^{-1}.

In the previous study we observed an abrupt drop in [NF(a)] upon the addition of H_2 (or D_2), followed by a very slow decay with further addition of H_2. We know now that the abrupt decrease in NF(a) was associated with the backflow of H_2 into the prereactor with removal of F atoms. With the improved inlet design (for large flows), the quenching kinetics for H_2 were better behaved and the rate was found to be much slower. The previous results for H_2 and D_2 should be disregarded. Due to the expense associated with high flows of D_2, the rate constant for D_2 was not remeasured. The poorly behaved quenching plots with HCl and COS were previously noted;[6] the [NF(a)] would drop upon introduction of HCl, but additional quenching with further added [HCl] was minor. The HCl and OCS reactions were restudied by using the modified reagent inlet, and the problem just mentioned no longer existed for HCl. The new data for HCl are as reliable as for other reagents; the value of k_{HCl} is a factor of 2 smaller than k_{HF}. The COS quenching plots were still poorly behaved and were the same for both types of reagent inlets and also for conditions of excess [F] or excess [N_3]. We assigned the rate constant for COS to be $(6 \pm 2) \times 10^{-14}$ cm^3 s^{-1} based upon the second, slow part of the quenching plot.

The rate constants for the quenching of NF(a) by H_2O and D_2O, see Figure 8, were difficult to measure because of the low vapor pressure of water. The reagents were loaded from fresh liquid samples after saturating and exchanging the surface of the glass lines and storage bulb overnight. Fresh reagent was then reloaded to slightly less than the room temperature vapor pressure. Because the low vapor pressure limited the reagent concentrations and, hence, the degree of quenching, the experimental error is 20–30% for k_{H_2O} and k_{D_2O}. The isotopic effect is small with $k_{H_2O}/k_{D_2O} \sim 1.2$.

The rate constants for small organic molecules and SF_6 are summarized in Table III. The organic reagents were subjected to freeze–pump–thaw cycles and stored in glass containers that were covered with a black cloth. Except for CF_4 and the alkanes, the rate constants are larger than for diatomic and triatomic molecules. The alkane systems have a behavior similar to H_2 and the open reagent inlet tube was required to obtain reliable data. The new rate constant for C_3H_8 is considerably smaller than the earlier approximate value.[6] Several experiments were done with C_2H_6 and CH_4. For the former, a significant degree of quenching could be obtained and a rate constant is quoted. However, the result for CH_4 is given as an upper limit because the degree of quenching was small even for the highest concentrations that were practical ($\sim 10^{15}$ molecules cm^{-3}). The rate constant for CH_3CN

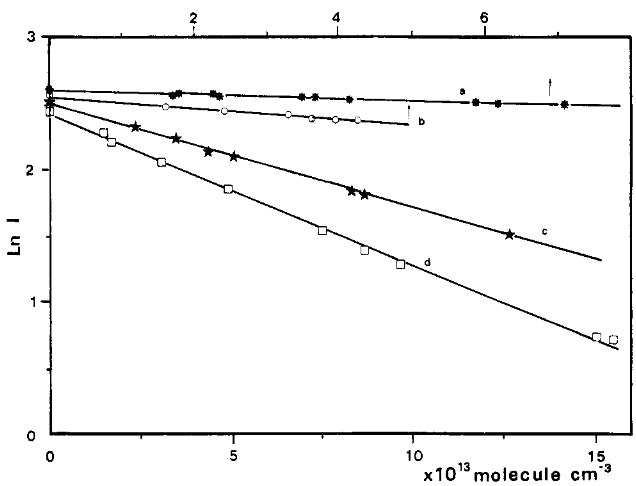

Figure 8. Pseudo-first-order NF(a) quenching plots for H_2O (*), D_2O (○), CH_3OH (★), and CH_3OD (□) with reaction times of 106, 35, 79, and 83 ms, respectively. The units of the upper and lower concentration scales are the same.

is small, and it is listed with the saturated alkanes. There was no isotope effect on the quenching rate constant for CD_3CN, in contrast to the large isotope effect found for quenching of NF(b) by CH_3CN and CD_3CN.[20] Figure 7 illustrates the increase in the rate constants for CH_3I vs CH_3Br. The trend of increasing k_Q with Cl, Br, and I holds also for the methylene halides and the trifluoromethyl halide series. As might be anticipated because k_{CH_4} is smaller than k_{H_2O}, the rate constant for CH_3OH is similar to k_{H_2O}.

The quenching rate constants for the unsaturated organic molecules are tabulated in the lower part of Table III. The rate constants for C_2H_4 and C_2H_2 are similar, $(32 \pm 3) \times 10^{-14}$ and $(23 \pm 2) \times 10^{-14}$ cm^3 s^{-1}, resepctively. However, the rate constants for propene and butadiene are considerably larger. The rate constants for acetone and acetone-d_6 resemble those for C_2H_4, suggesting quenching by addition to the C═O bond. The quenching rate constant for CF_3COOH, 57×10^{-14} cm^3 s^{-1}, is larger than for CH_3OH, but resembles that for $(CH_3)_2CO$, which suggests that the C═O bond may be involved in quenching as well as the hydroxy group. On the other hand, perfluoroacetone has a very small rate constant. An initially surprising result was the large rate constant for $(CH_3)_2O$, given the modest rate constant for CH_3OH. However, experiments with $(C_2H_5)_2O$ confirmed the large quenching rate constants for ethers.

A systematic study was made of quenching by ammonia, amines, and other group V elements containing hydrogen and methyl groups. The results are summarized in Table IV and some quenching plots are shown in Figure 9. Since the rate constants are 1–2 orders of magnitude greater than for other molecules, the flow distance for measuring the decay rate of NF(a) was shortened, [Q] reduced, or both. Diluting the reagent with an inert

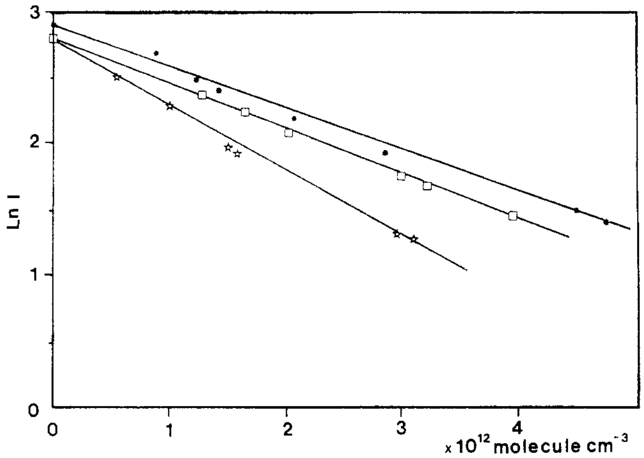

Figure 9. Pseudo-first-order NF(a) quenching plots versus concentration for three amines: (□, CH_3NH_2) Δt = 21 ms; (*, $(CH_3)_2NH$) Δt = 19 ms; (☆, $N(CH_3)_3$) Δt = 21 ms.

gas can be used to reduce [Q], but adsorption of NH_3 or amines on the walls of the glass reservoir may reduce the reagent concentration. To address these problems, rate constants derived from long reaction times with freshly prepared dilute mixtures were compared to measurements with pure gases at short reaction times. The new data give rate constants for NH_3 and $N(CH_3)_3$ that are twice as large as the earlier report.[6] We repeated the experiment several times using the methods discussed above, and the data seemed to be reproducible. We believe that the low values from the previous report are a consequence of adsorption of the reagent upon the reservoir walls from the dilute mixtures (1%) used in that work. Experiments were done with ND_3 to test for a possible kinetic isotope effect. In order to avoid exchange with the walls, the reservoir and lines first were seasoned with D_2O, then the ND_3 mixture was prepared and stored. Within the uncertainty of the measurements, there was no isotope effect upon k_{NH_3} vs k_{ND_3}. The quenching rate constants for $N(CH_3)_3$, $P(CH_3)_3$, and $Bi(CH_3)_3$ are 2.6×10^{-11}, 2.3×10^{-11}, and 2.7×10^{-11} $cm^3\ s^{-1}$, respectively, which are 8 times larger than those for NH_3 and PH_3. The quenching rate constant for NH_3 was measured in both the coated and the uncoated reactor; the results were in good agreement.

In order to determine the quenching rate constant by HN_3, $[F]_0$ was selected to be $<2[HN_3]_0$, so that all the F atoms were removed but some N_3 remained. Then, HN_3 was added as reagent. Under such conditions, the unreacted N_3 and HN_3 from the prereactor act just as impurities, and the HN_3 added at the reagent inlet can be treated as any other quenching molecule. The least-squares analysis of the data gave $k_{HN_3} = (2.1 \pm 0.2) \times 10^{-13}$ $cm^3\ s^{-1}$.

(*5*) *Quenching Rate Constants at 196 K.* Rate constants were measured at 196 K for CO, O_2, and C_2H_4. The experiments were done by enclosing the reactor, but not the prereactor, in a cardboard box and then filling the box with solid CO_2 (dry ice). The reagents were metered to the reactor in the normal way. The first-order decay of NF(a) with and without added reagent was as expected, providing that the dependence of [Q] and reaction time on temperature was taken into account. The quenching plots were normal and the rate constants for CO, O_2, and C_2H_4 were $(5.2 \pm 0.5) \times 10^{-16}$, $(2.8 \pm 0.3) \times 10^{-15}$, and $(1.6 \pm 0.2) \times 10^{-13}$ at 196 K. These experiments demonstrated that the NF(a) kinetics in the wax-coated reactor were well-behaved at 196 K. Unfortunately, the halocarbon wax has a low melting point, ~340 K, and heating the present reactor is not possible. The 7-fold reduction in rate constant for CO is very suggestive that this reaction proceeds over a repulsive barrier in the entrance channel. The smaller reductions found for the rate constants of the other two reactions are less easy to interpret.

Discussion

(*1*) *NF(a) Decay Processes in the Absence of Q.* Deactivation of NF(a) by collisions with the halocarbon wax coated Pyrex walls was minor. However, quenching by uncoated Pyrex walls was significant, and precautions against deactivation by collisions with the surface of the reactor must be considered when studying NF(a). The experiments at 196 K demonstrated that the 2F + HN_3 source can be used for low-temperature studies, as well as for room-temperature work. A Teflon coated reactor might be suitable for high-temperature experiments. Examination of the [NF(a)] profile along the flow reactor in the presence of excess F confirmed that the reaction rate of F atoms with N_3 is fast. Although these experiments were not designed to measure k_2, the best fit to the current data at 300 K seems to be $(4.0 \pm 1.0) \times 10^{-11}$ $cm^3\ s^{-1}$. Quenching by F atoms and HN_3 have rate constants of (4 and 2) $\times 10^{-13}$ $cm^3\ s^{-1}$, respectively. Although the pressure dependence was not studied here, quenching by F atoms could be third order and proceed via an excited NF_2^* potential. The rate constant for HN_3 is much smaller than the analogous reaction of NH(a) with HN_3 (1.2×10^{-10} $cm^3\ s^{-1}$), which mainly occurs by H abstraction.[10] Another contrast to NH(a) was the absence of observable emission from NHF* in the NF(a) reaction with HN_3.

If $[NF(a)] \gtrsim 1.0 \times 10^{12}$ molecules cm^{-3}, bimolecular self-destruction gives a noticeable decay of [NF(a)] and the rate constant was assigned as $(5 \pm 2) \times 10^{-12}$ $cm^3\ s^{-1}$ at a total pressure of 2.7 Torr. In order to test for a possible three-body contribution to bimolecular destruction, some experiments were done at 7.5 Torr. We found no significant (±30%) effect upon the rate constant. The total bimolecular rate constant is somewhat larger than our previous estimate using the same technique. A rate constant of this magnitude also has been found by Benard and co-workers.[27a] Bimolecular energy pooling to generate NF(b) is a minor component of the total bimolecular decay. The exit channels for the self-destruction reaction have not been established; stepwise deactivation to NF(X) + NF(a) or chemical reaction giving N_2 are possibilities. The large rate constant for self-destruction, the absence of NF(a) dimols emission, and the small k_{EP} suggest that the $N_2F_2^*$ potentials arising from 2NF(a) interact more strongly with repulsive potentials from 2NF(X) or NF(X) + NF(a) rather than those from NF(X) + NF(b). Heidner and co-workers have reported that the NF(X) + NF(X) rate constant is $<5 \times 10^{-12}$ $cm^3\ s^{-1}$.[27b]

(*2*) *NF(a) Quenching by Small Molecules: E–V Transfer.* The small rate constants in Table II imply that quenching by most diatomic molecules is by an E–V mechanism. Deactivation to NF(X) is exoergic by 11 441 cm^{-1}, and several vibrational quanta may be excited, depending on the reagent. Deactivation of NF(b) to NF(a) releases 7570 cm^{-1} and only two to four vibrational quanta may need to be excited.[20] In spite of this energy difference, the quenching rate constants for diatomic and triatomic molecules tend to be in the 10^{-15}–10^{-14} $cm^3\ s^{-1}$ range for both NF states. In contrast, the rate constant for $O_2(a)$ with only 7880 cm^{-1} of energy is 4 orders of magnitude smaller. The approach of NF($a^1\Delta$) to a closed shell reagent molecule generates two potentials, $^1A'$ and $^1A''$. The former, which arises from the $\pi_x^2-\pi_y^2$ component of NF(a), generally will be attractive and correlate to the ground electronic state of the Q–NF molecule; the $^1A''$ potential, which arises from the $\pi_x\pi_y$ component and correlates to a singlet excited Q–NF state, is repulsive. The E–V mechanism for quenching could be a physical process involving coupling to vibrational energy states on the repulsive potential or a "chemical" mechanism involving the attractive potential. If the bound $^1A'$ ground-state potential (H_2NF, FN_3, FNCO, or HNF_2 for example) crosses the $NF(X^3\Sigma^-)$ + Q exit channel potential, E–V quenching would be faster than for the physical mechanism. In this sense the mechanism for E → V quenching of NF(a) probably differs from that for NF(b) or O_2(a or b), which is usually modeled as collision-induced E–V transfer on repulsive entrance and exit channel potentials that do not cross.[20] The physical mechanism is associated with a strong correlation between the magnitude of the rate constant and the highest stretching vibrational frequency

(27) (a) Benard, D. J.; Winker, B. K.; Seder, T. A.; Cohn, R. H. *J. Phys. Chem.* **1989**, *93*, 4790. (b) Heidner, R. F.; Helvajian, H.; Holloway, J. S.; Koffend, J. B. *J. Phys. Chem.* **1989**, *93*, 7513.

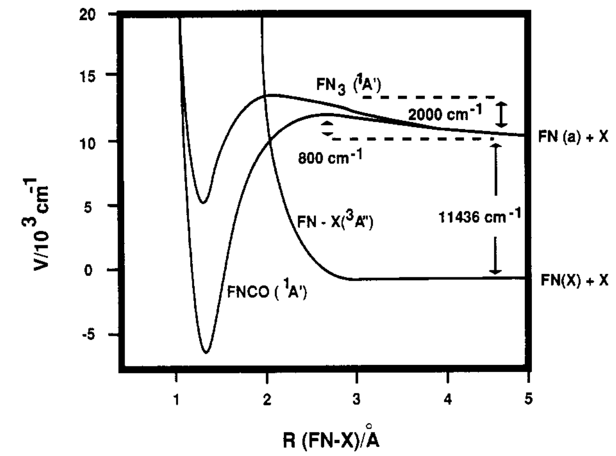

Figure 10. Schematic potential energy profiles for quenching of NF(a) by CO and N_2. The $^1A'$ potentials were sketched by using a Morse form plus added barrier (see text). The repulsive triplet potential was obtained from a Lennard-Jones potential with parameters from O_2 and N_2(CO) but shifted to smaller r to account for the bond lengths of N_2(CO) and NF. The repulsive $^1A''$ potential that arises from the $\pi_x\pi_y$ component of NF($a^1\Delta$) is not shown. See text for method of assignment of the barriers.

of the molecule and large hydrogen–deuterium kinetic isotope effects.

Schematic potentials for the $^1A'$ entrance channel and $^3A''$ exit channel for the NF(a) + N_2 (or CO) systems are illustrated in Figure 10. These potentials were estimated using a Morse representation of the FN–CO or FN–N_2 bond with assumed values for D_e, R_e, and ω_e. This sketch is consistent with ab initio potentials for HN_3[28] and FN_3.[29] The repulsive potential correlating to NF($X^3\Sigma^-$) was assigned from Lennard-Jones constants for O_2–CO with substraction of 0.5 Å to account for the bond lengths of O_2 and CO. The barrier (~3 kcal mol^{-1}) shown for FNCO($\tilde{X}$) was assigned from the temperature dependence of k_{CO}. The barrier for FN_3($\tilde{A}$) was set at ~7 kcal mol^{-1} to be consistent with the relative values of k_{CO} and k_{N_2}. Additional insight for the FN_3 and FNCO potentials can be gained by considering the products from the F + N_3 and F + NCO reactions. The F + N_3 reaction seems to occur entirely on the $FN_3(\tilde{X}^1A')$ potential and generate NF(a) in high yields, which is consistent with a crossing of the $FN_3(\tilde{a}^3A'')$ potential at long range. This location also is favored from ab initio calculations.[29] The failure of the F + NCO reaction to give NF(a) + CO has been interpreted as a thermochemical limitation.[31] This result and the larger D(FN–CO) suggest that the FNCO($^3A''$) potential probably crosses the $^1A'$ potential inside the barrier, as shown in Figure 10. After a NF(a) + CO collision surmounts the barrier, the vibrationally excited FNCO ($\tilde{X}$,$^1A'$) molecule will either redissociate or cross the the $^3A''$ potential and give NF($X^3\Sigma^-$). The larger NF(a) quenching rate constant for CO, relative to N_2, mainly arises as a consequence of the smaller barrier for FN–CO($\tilde{X}^1A'$) vs FN–N_2($\tilde{X}^1A'$), according to the view of Figure 10. The larger (10^4) quenching rate constant for NH(a) vs NF(a) by CO and N_2[10e,f] is consistent with smaller barriers and crossings with the triplet exit channel inside the barrier for HN_3 and HNCO.[28b] The difference in rate constants for CO and N_2 is maintained for both NH(a) and NF(a).

The schematic potential energy diagram in Figure 10 also can serve as reference for other systems in which NF(a) + Q correlates to a ground-state Q·NF molecule. Since NF(a), in fact, is formed in very high yield from the H + NF_2 reaction via HF elimination from $NF_2H(\tilde{X}^1A')$,[1a] NF(a) + HF must correlate with the $NF_2H(\tilde{X},^1A')$ potential. For the reverse reaction, the critical question is the height of the barrier and the location of the crossing position between the $NF_2H(\tilde{X},^1A')$ and $NF_2H(\tilde{a}^3A'')$ potentials. For three-centered HF and HCl unimolecular elimination reactions, the threshold energy is usually 5–15 kcal/mol in excess of the reaction endoergicity;[31] a 5–10 kcal/mol barrier for the quenching of NF(a) by HF is consistent with our 300 K rate constant. Quenching could occur via impulsive collisions between HF and NF(a) on the repulsive parts of the $^1A'$ or $^1A''$ potentials at long range, as for O_2(a) and NF(b) interacting with HF.[12b,20] Alternatively, quenching involves transfer from the $\tilde{X}^1A'$ surface to the $^3A''$ surface at the crossing seam. If the crossing position for NF_2H was inside the barrier, as shown for FN–CO in Figure 10, then the high branching ratio for NF(a) formation from H + NF_2 would not be expected. Therefore, the crossing position must be close to the top or even outside the barrier. The mechanism for quenching by HCl should resemble that for HF. Quenching by H_2 can be discussed in the same framework with NH_2F being the stable molecule; the small value for k_{H_2} implies a large barrier in the $\tilde{X}^1A'$ potential. In this case, formation of NH(a or X) + HF, as well as NF(X) + H_2, are possible exit channels from $FNH_2(X^1A')$. Quantitative information about exit channels for FNH_2 prepared by F + NH_2 is not available but both NH(X) and NH(a) seem to be products.[32,33]

The rate constant for NF(a) + NO is 4 orders of magnitude smaller than for NH(a) + NO and there must be one (or more) barriers to the exoergic N_2O + F exit channel. The NH(a) reaction with NO is chemical in nature and little NH(X) is formed.[10e]

These qualitative observations point to the importance of gaining an understanding of the NF–Q($\tilde{X}^1A'$) potentials, including the barrier and the interaction with the $\tilde{a}^3A''$ potentials, as the key for describing the quenching of NF($a^1\Delta$) by small molecules. There is a need for some calculated potentials of model systems for the $^1A''$, $^1A'$, and $^3A''$ states. Experimental determination of the activation energies for quenching should provide the barrier heights in the entrance channel. Comparisons of the rate constants in Table II with those for NH(a) indicate that the barrier in the entrance channels generally is larger for NF(a) than for NH(a). This is consistent with the small barriers calculated for NH(a) reactions.[10d,10i]

The deactivation of NF(a) by O_2 with a rate constant of 6.6 × 10^{-15} cm^3 s^{-1} probably proceeds by excitation transfer

$$\mathrm{NF(a)} + \mathrm{O_2(X)} \rightarrow \mathrm{NF}(X, v''=0) + \mathrm{O_2}(a, v'=0);\ \Delta H_0^\circ = -3500\ \mathrm{cm^{-1}}$$

The modest reduction in k_{O_2} at 196 K implies a curve-crossing position on the repulsive wall of the V(NF(a)–O_2) entrance channel potential. Although the electron exchange process between NF(a) and O_2 may circumvent spin restrictions,[34] the nonresonance energy transfer and unfavorable Franck–Condon factors for vibrational excitation of either NF(X) or O_2(a) contribute to the small rate constant. Another reagent that probably quenches by excitation transfer is CF_3NO. The quenching rate constant of NH(a) by O_2 has been revised downward[10e,f] and (4.5–6.2) × 10^{-14} cm^3 s^{-1} is favored now. The concomitant formation of NH(X) and O_2(b) has been demonstrated and the NH(a) reaction proceeds by excitation transfer (ΔH_0° = −433 cm^{-1}).

(3) *Quenching of NF(a) by Polyatomic Molecules: Chemical Reaction.* The rate constants for organic molecules vary from 10^{-11} to 10^{-14} cm^3 s^{-1} and comparisons with O(^{1}D), NH($a^1\Delta$), and $CH_2(\tilde{a}^1A_1)$ are helpful. Insertion into C–H bonds and addition to double bonds are typical reactions for these species. Chemical reaction is dominant over physical deactivation, but recent work shows that physical deactivation exists (~20%) even for CH_2($\tilde{a}^1A_1$) with olefins.[11d] Abstraction of H also has been detected

(28) (a) Stephenson, J. C.; Casassa, M. P.; King, D. S. *J. Chem. Phys.* **1988**, *89*, 1378. (b) Alexander, M. H.; Werner, H. J.; Dagdigian, P. J. *Chem. Phys.* **1988**, *89*, 388.
(29) Michels, H. H. United Technologies Research Center, Hartford, CT, private communication.
(30) Du, K. Y.; Setser, D. W. *Chem. Phys. Lett.* **1988**, *153*, 393.
(31) (a) Schug, K. P.; Wagner, H. G.; Zabel, F. *Ber. Bunsen-Ges. Phys. Chem.* **1979**, *83*, 167. (b) Sudbo, Aa. S.; Schulz, P. A.; Shen, Y. R.; Lee, Y. T. *J. Chem. Phys.* **1978**, *69*, 2312. (c) Holmes, B. E.; Setser, D. W.; Pritchard, G. O. *Int. J. Chem. Kinet.* **1976**, *8*, 215.
(32) Wategaonkar, S.; Setser, D. W. *J. Chem. Phys.* **1987**, *86*, 4477.
(33) Donaldson, D. J.; Sloan, J. J.; Goddard, J. D. *J. Chem. Phys.* **1985**, *82*, 4524.
(34) Jones, I. T. N.; Bayes, K. D. *J. Chem. Phys.* **1972**, *57*, 1003.

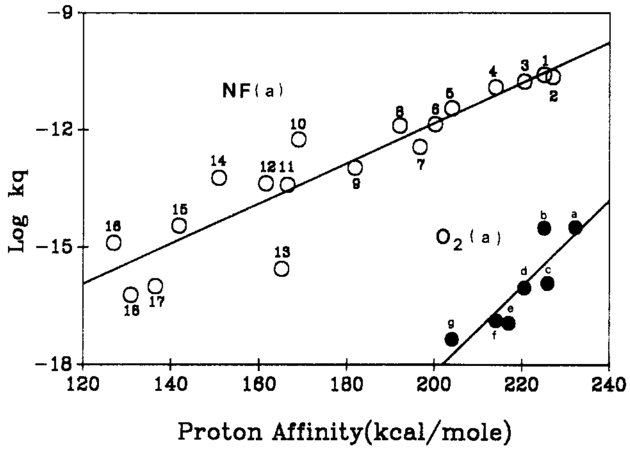

Figure 11. Plot of k_Q vs the proton affinities of reagent molecules containing either N or O atoms. The proton affinities were taken from ref 37b. The rate constants are as follows: 1, $N(CH_3)_3$; 2, $P(CH_3)_3$; 3, $NH(CH_3)_2$; 4, NH_2CH_3; 5, NH_3; 6, $(C_2H_5)_2O$; 7, $(CH_3)_2CO$; 8, $(CH_3)_2O$; 9, CH_3OH; 10, CF_3COOH; 11, H_2O; 12, SO_2; 13, $(CF_3)_2CO$; 14, COS; 15, CO; 16, NO; 17, CO_2; 18, N_2O. The correlation plot in the lower part of the figure is for O_2(a); the reagents are as follows: a, $N(C_2H_5)_3$; b, $N(CH_3)_3$; c, $NH(C_2H_5)_2$; d, $NH(CH_3)_2$; e, $NH_2C_2H_5$; f, NH_2CH_3; g, NH_3.

for $O(^1D)$, $CH_2(\tilde{a}^1A_1)$, and $NH(a^1\Delta)$.[10,11] Abstraction of halogen is documented for $CH_2(\tilde{a}^1A_1)$ and $O(^1D)$, but halogen abstraction by NH(a) has not been proven. Several mechanisms have been proposed for the reaction of O_2(a) with unsaturated molecules, including dioxetane and hydroperoxide formation.[35,36] The proof of the dioxetane scheme came from observing CH_2O chemiluminescence. Addition of NF(a) to unsaturated molecules giving a three-membered ring, which subsequently would decompose or isomerize to more stable products, would be expected.

The quenching rate constant of NF(a) by CH_4 is much smaller than for NH(a), but the rate constants increase systematically with substitution by heavier halogen. The change seems too large to be explained by any effect related to the decrease in electronegativity for Cl, Br, and I (3.0, 2.8, and 2.5, respectively). More likely, the quenching mechanism involves direct interaction of NF(a) with the halogen atoms by abstraction or insertion. The absence of a significant C–H/C–D kinetic isotope effect also emphasizes the importance of interaction with the C–X bond. The similar trend for the halogenated fluoromethanes also may be attributed to an insertion or abstraction mechanism. The C–F bond itself is inert to quenching. The mechanism with alkanes probably is C–H insertion, but with a significant barrier. Vibrationally excited CH_3–NHF type molecules will decompose by unimolecular HF elimination.

The increase in the rate constants with methyl substitution of NH_3 implies that NF(a) interacts with the electron pair, which becomes increasingly basic in this amine series. Gas-phase proton affinity values are a good measure of base strength. As a general test of the possibility that quenching involves interaction of NF(a) with an electron pair on the reagent, the quenching rate constants are plotted vs the proton affinity[37] values of several reagents in Figure 11. A rather good correlation exists for molecules containing oxygen and nitrogen, although the compression in plot resulting from a log k_Q scale should be remembered. Surprisingly, the points for NO and CO even fall close to the correlation line, which covers nearly 4 orders of magnitude in k_Q. This correlation strongly suggests the importance of a Lewis acid–base type interaction between the $\pi_x^2-\pi_y^2$ component of NF(a) and an electron pair of the reagent as the dominant factor in determining the barrier heights in the NF–Q($^1A'$) entrance channel potential.

(35) Bogan, D. J.; Durant, J. L.; Sheinson, R. S.; Willilams, F. W. *Photochem. Photobiol.* **1979**, *30*, 3.
(36) Bogan, D. J. *Chemical and Biological Generation of Excited States*; Adam, W., Cilento, G., Eds.; Academic Press: New York, 1982; p 37.
(37) Lias, S. G.; Liebman, J. F.; Levin, R. D. *J. Phys. Chem. Ref. Data* **1984**, *13*, 695.

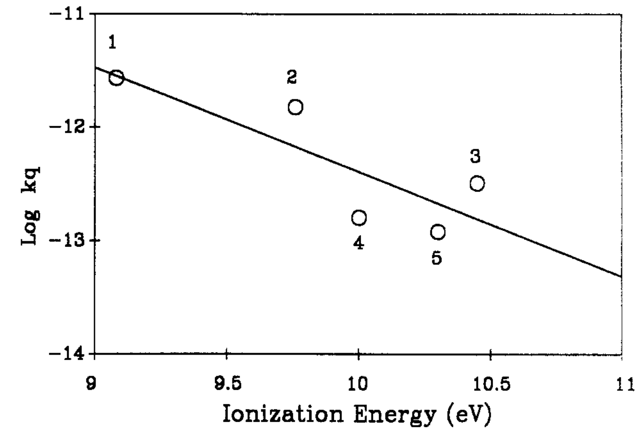

Figure 12. Correlations plot between the ionization energies of olefins and their quenching rate constants for NF(a): 1, C_4H_6; 2, C_3H_6; 3, C_2H_4; 4, CH_2CHCl; 5, CH_2CF_2.

After the barrier is crossed, energy will be released and the subsequent chemical rearrangements of the Q:NF adducts are not so easy to predict. The lack of significant kinetic isotope effect for H_2O/D_2O and for NH_3/ND_3 also is consistent with a chemical interaction leading to adduct formation. The fact that the correlation plot includes CO and NO suggests that overcoming the barrier shown in Figure 10 is the rate-limiting step and that crossing to the triplet surface is favored over dissociation of NO:NF* or CO:NF*. The rate constants for H_2S (PA = 170 kcal mol^{-1}) and PH_3 (PA = 189 kcal/mol) are above the correlation line and insertion or abstraction with the S–H and P–H bonds, as well as adduct formation, is implied. The rate constants of CO_2 and N_2O fall below the correlation line, but k_{COS} is slightly above the line. The proton affinity of $(CF_3)_2CO$ is smaller than for $(CH_3)_2CO$, but the rate constant for $(CF_3)_2CO$ is far below the correlation line. After the correlation between k_Q and base strength was discovered, this small rate constant was confirmed by an independent check. Perfluoroacetone may be a case for which there are no exoergic chemical reaction channels for the adduct $((CF_3)_2CO{:}NF)^*$ and a competition develops between redissociation and crossing to the triplet channel (as for CO and NO). Another strong base, CH_3CN (PA = 188.4 kcal mol^{-1}), has a rate constant that is 2 orders of magnitude smaller than that predicted by the correlation. After all other experiments were fone, the rate constant for CH_3CN was reinvestigated at 3 and 7.5 Torr. The value in Table III was confirmed and there was no dependence on Ar pressure. We suspect that adduct formation $(H_3CN{:}NF)^*$ does occur, but subsequent chemical reaction is not facile and competition between crossing to the triplet state and redissociation occurs. The small rate constant could reflect just the quenching from the interaction with the C–H bonds of CH_3CN.

The enhanced quenching rate constants of O_2(a) by substituted amines has been explained by Ogryzlo and Tang[38] in terms of a "charge-transfer" mechanism, since the trend in rate constants correlated with the ionization energies of substituted amines. However, the O_2(a) rate constants also correlate with the proton affinities of the amines, as shown by the plot in the lower part of Figure 11. The O_2(a) state also seems to exhibit an electron pair acceptor capability with these reagents. Both the proton affinities and the ionization energies measure the relative base strengths of the amines, which reflect the change in barrier heights to adduct formation.

A correlation exists between the rate constants for olefins and their ionization energies, see Figure 12, with the rate constants being larger for molecules with smaller ionization energy. The general increase in rate constant also follows the increase in proton affinity for the series; but, the correlation line does not match the

(38) Furukawa, K.; Ogryzlo, E. A. *J. Photochem.* **1972/1973**, *1*, 163. These authors use the term "charge-transfer" to describe the partial donation of an electron pair from an amine to the oxygen molecule. This implies the same concept as our acid–base adduct.

one in Figure 11 and the correlation fails for CH_2CHCl and CH_2CF_2. Carbenes, especially $SiCl_2$, exhibit a similar ordering of rate constants for this series of olefins.[39-41] The increase in rate constants of singlet carbenes with methyl substitution of C_2H_4 has been interpreted as a consequence of inductive donation of electrons to the π system by methyl. Thus, the π system more readily coordinates with the vacant p orbital of the singlet carbene. Conversely, halogen substitution withdraws electrons from the π system and reduces the rate constants. These rather complicated electronic effects are approximately represented by the trend in ionization energies.[41] This correlation for the rate constants of $NF(a^1\Delta)$ confirms a carbenelike reactivity and evidently the π system of the olefin donates an electron pair to the vacant orbital of the $\pi_x^2-\pi_y^2$ component to initiate the addition reaction of NF(a). Just as for carbene reactions, this step is followed by interaction of the electron pair initially on NF(a) with the olefin to complete the addition reaction.

Conclusions

The room temperature quenching rate constants for NF(a) span a range from $\sim 1 \times 10^{-17}$ for N_2 to 2.6×10^{-11} cm^3 s^{-1} for trimethylamine and trimethylbismuth. In general, the quenching rate constants are not so large as to preclude using NF(a) as a gas-phase energy storage molecule. A comprehensive correlation was found between the quenching rate constants and the proton affinity values for reagent molecules that can act as bases, i.e., those containing oxygen and nitrogen. A less extensive correlation was found between the rate constants and the ionization energies for alkenes. These correlations and the absence of any H/D kinetic isotope effect upon the rate constants strongly suggest that chemical interactions control the quenching rate, rather than a physical E-V quenching mechanism. The correlation of rate constants with base strengths of the reagent implies that the $\pi_x^2-\pi_y^2$ component of the NF(a) structure is more important than the $\pi_x\pi_y$ biradical component, as is expected from the ordering of the $^1A'$ and $^1A''$ potentials correlating to $NF(a^1\Delta)$ + Q. The quenching rate constants for NO and NO_2 are small, which is further evidence that the $\pi_x\pi_y$ component is not very reactive even with radicals. Considerable effort was expended to characterize the bimolecular self-quenching of NF(a), and a rate constant of $(5 \pm 2) \times 10^{-12}$ cm^3 molecule^{-1} s^{-1} is favored. Energy pooling to give NF(b) and NF(X) is a minor component to the self-quenching process. The products presumably are N_2 and F_2 (or 2F) or stepwise relaxation giving NF(X) and NF(a). The 2F + HN_3 reaction system was shown to be a suitable source for studies of NF(a) at 200 K, as well as at 300 K.

Acknowledgment. This work was supported by the U.S. Air Force Office of Scientific Research (Grant 88-0279). We thank Professor Dick McDonald for advice on the proton affinity correlation plot.

(39) Safarik, I.; Ruzsicska, B. P.; Jodhan, A.; Strausz, O. P.; Bell, T. N. *Chem. Phys. Lett.* **1985**, *113*, 71.
(40) Cha, J. O.; Beach, D. B.; Jasinski, J. M. *J. Phys. Chem.* **1987**, *91*, 5340.
(41) Baggott, J. E.; Blitz, M. A.; Frey, H. M.; Lightfoot, P. D.; Walsh, R. *J. Chem. Soc. Faraday Trans. 2* **1988**, *84*, 515.

A Laser Photolysis Study of the Reaction of SO_4^- with Cl^- and the Subsequent Decay of Cl_2^- in Aqueous Solution

W. John McElroy

Central Electricity Generating Board, National Power Division, Technology and Environmental Centre, Kelvin Avenue, Leatherhead, Surrey KT22 7SE, U.K. *(Received: July 11, 1988; In Final Form: December 2, 1988)*

Kinetic spectroscopic techniques were employed to investigate the reactions of the SO_4^- and Cl_2^- radicals following photolysis of $K_2S_2O_8$–NaCl solutions at 248 nm. The extinction coefficient of SO_4^- was estimated to have a value of $(1.6 \pm 0.1) \times 10^3$ M^{-1} cm^{-1} (base 10) at 450 nm, its wavelength of maximum absorbance. A mechanism is proposed which accounts for the observed decay of Cl_2^- in aqueous solution. Several rate coefficients have been determined at 20 °C: $k(SO_4^- + Cl^-) = (2.7 \pm 0.4) \times 10^8$ M^{-1} s^{-1} (at zero ionic strength), $2k(Cl_2^- + Cl_2^-) = (1.4 \pm 0.2) \times 10^9$ M^{-1} s^{-1} (at zero ionic strength), $k(Cl_2^- + H_2O) = (1.3 \pm 0.1) \times 10^3$ s^{-1}, and $k(Cl + H_2O) = (2.5 \pm 0.2) \times 10^5$ s^{-1}.

Introduction

The aqueous oxidation of SO_2 to form sulfuric acid is of fundamental importance in the atmosphere since this process exerts a considerable influence on the composition and, in particular, the acidity of cloud and rainwater.[1] Many uncertainties still remain with regard to the kinetics and mechanisms of SO_2 oxidation,[2,3] and their elucidation is particularly important if experimental measurements are to be extrapolated to atmospheric conditions which are much more complex than simpler laboratory systems.

It has been proposed that radicals such as SO_3^-, SO_4^-, and SO_5^- are key intermediates in the autoxidation of aqueous solutions of SO_2.[4] While the available literature on this process is extensive, the mechanism has yet to be fully resolved.[3,5] Chloride ion is a major component of cloud and rainwater in maritime air masses. Reaction of the SO_4^- radical with Cl^- leads to the production of the dichloride ion, Cl_2^-.[6]

$$SO_4^- + Cl^- \rightarrow SO_4^{2-} + Cl \quad (1)$$

$$Cl + Cl^- \rightleftarrows Cl_2^- \quad (2')$$

The impact of chloride ion on the rate of SO_2 oxidation is dependent on the subsequent fate of the Cl_2^- radical and also the mechanism of the autoxidation reaction itself.[3,5]

Kinetic studies of the reaction of SO_4^- with Cl^- have been carried out previously using flash photolysis or pulse radiolysis techniques.[6-10] Under second-order conditions the accuracy of

(1) Scire, J. A.; Venkatram, A. *Atmos. Environ.* **1985**, *19*, 637.
(2) Hoffmann, M. R.; Jacob, D. J. *SO_2, NO and NO_2 Oxidation Mechanisms: Atmospheric Considerations*; Butterworth: Boston, 1984; Chapter 3.
(3) McElroy, W. J. *Atmos. Environ.* **1986**, *20*, 323.
(4) Hayon, E.; Treinen, A.; Wilf, J. *J. Am. Chem. Soc.* **1972**, *94*, 47.
(5) Huie, R. E.; Neta, P. *Atmos. Environ.* **1987**, *21*, 1743.
(6) Chawla, O. P.; Fessenden, R. W. *J. Phys. Chem.* **1975**, *79*, 2693.
(7) Chawla, O. P. An Electron Spin Resonance Study of Photochemical Reactions in Aqueous Solutions. Ph.D. Thesis, Carnegie-Mellon University, Pittsburgh, 1973.

0022-3654/90/2094-2435$02.50/0